

Constraints on 3.55 keV line emission from stacked observations of dwarf spheroidal galaxies

D. Malyshev, A. Neronov, and D. Eckert

Department of Astronomy, University of Geneva, ch. d'Ecogia 16, CH-1290 Versoix, Switzerland

Several recent works have reported the detection of an unidentified X-ray line at 3.55 keV, which could possibly be attributed to the decay of dark matter (DM) particles in the halos of galaxy clusters and in the M31 galaxy. We analyze all publicly-available XMM-Newton data of dwarf spheroidal galaxies to test the possible DM origin of the line. Dwarf spheroidal galaxies have high mass-to-light ratios and their interstellar medium is not a source of diffuse X-ray emission, thus they are expected to provide the cleanest DM decay line signal. Our analysis shows no evidence for the presence of the line in the stacked spectra of the dwarf galaxies. It excludes the sterile neutrino DM decay origin of the 3.5 keV line reported by Bulbul et al. (2014) at the level of 4.6σ under standard assumptions about the Galactic DM column density in the direction of selected dwarf galaxies and at the level of 3.3σ assuming minimal Galactic DM column density. As a by-product of our analysis, we provide updated upper limits to the mixing angle of sterile neutrino DM in the mass range between 2 and 20 keV.

I. INTRODUCTION

In a recent work, Bulbul et al. [1], Boyarsky et al. [2] reported the detection of an unidentified 3.55 keV line in the analysis of stacked data on galaxy clusters observed by XMM-Newton, in the observations of individual galaxy clusters (Perseus) and in the Andromeda galaxy. In the absence of obvious options for this line to be of instrumental/astrophysical origin (see, however, Jeltema and Profumo [4]), the authors invoked the possibility for the line to be produced in the decay of Dark Matter (DM) particles populating the halos of the considered structures. Assuming a sterile-neutrino nature of the decaying DM (see e.g. Dodelson and Widrow [5], Asaka et al. [6], Lattanzi and Valle [7] and references therein), Bulbul et al. [1] obtained a value of $\sin^2(2\theta) \sim 6.8 \times 10^{-11}$ for the the mixing angle of the sterile neutrino and a particle mass m_{DM} of 7.1 keV. These parameters are consistent with the previously-derived upper bounds on $\sin^2(2\theta)$ from observations of the extragalactic diffuse X-ray background [9, 10]; galaxy clusters [11–13]; the Milky Way, Andromeda (M31) and Triangulum (M33) galaxies [10, 11, 14–18] and individual dwarf spheroidal (dSph) satellites of the Milky Way [15, 19–24].

The signal from decaying DM is expected to be strongest from the most nearby source, our own Milky Way galaxy. However, the signal is distributed over the entire sky, so that it is not straightforward to look for this signal using narrow-field X-ray telescopes. Besides, the radial density profile of DM in the Milky Way is somewhat uncertain, especially in its central part, where a significant contribution to the overall matter content of the Galaxy comes from the baryons. Recently Riemer-Sorensen [25] analyzed Chandra data on the Galactic Center (GC) region, finding no clear evidence for the 3.55 keV line (see however Boyarsky et al. [3]). The non-detection of the signal from the GC was found to be consistent with the existence of the DM sterile neu-

trino with parameters suggested by Bulbul et al. [1] for the most conservative assumptions on the DM density profile in the innermost part of the Galaxy.

The signal from the Milky Way halo is superimposed on approximately equally strong signal from the DM halos of nearby dSph galaxies in the direction of these sources. Combining the two signals and additionally stacking the signal from all the observed dSph systems, an improved sensitivity to the DM decay line can be obtained compared to the previously-reported constraints from the Milky Way or individual dSph galaxies.

In the following, we perform a stacked analysis of dSph galaxies using XMM-Newton data. In spite of a shorter overall exposure compared to the stacked galaxy cluster dataset analyzed by Bulbul et al. [1], the signal from the dSph is cleaner than in galaxy clusters, because the interstellar medium of dSph galaxies is not a source of thermal X-ray emission, contrary to the intracluster medium of the galaxy clusters. The work presented here is organized as follows. In the next section, we discuss the expected flux level from the dSph galaxies (Sect. II A) and the contribution of the Milky Way (MW) halo to the observed signal in Sect. II B. The details of the XMM-Newton observations and of the analysis procedure are given in Sect. III. Finally, the results are summarized and discussed in Sect. IV.

II. EXPECTED SIGNAL FROM DM DECAY

A. dSph galaxies

The decay of DM particles of mass m_{DM} results in a line at the energy $\epsilon = m_{DM}/2$ and flux

$$F = \frac{\Gamma M_{DM, FoV}}{4\pi d^2 m_{DM}} \quad (1)$$

where $M_{DM, FoV}$ is the total DM mass within the field of view (FoV) of the telescope. In the case of sterile

neutrinos, the radiative decay width Γ can be written as [26]

$$\begin{aligned} \Gamma &= \frac{9\alpha G_F^2}{256 \cdot 4\pi^4} \sin^2 2\theta_{DM} m_{DM}^5 \\ &\simeq 1.7 \times 10^{-28} \left[\frac{\theta_{DM}^2}{1.75 \times 10^{-11}} \right] \left[\frac{m_{DM}}{7.1 \text{ keV}} \right]^5 \text{ s}^{-1} \end{aligned} \quad (2)$$

where we have normalized the mixing angle θ_{DM} and m_{DM} to the values reported in Bulbul et al. [1]. Substituting this expression into Eq. 1 one finds the flux from dwarf spheroidal in the field of view to be

$$\begin{aligned} F_{dSph} &\simeq 2.4 \times 10^{-7} \left[\frac{\theta_{DM}^2}{1.75 \times 10^{-11}} \right] \left[\frac{m_{DM}}{7.1 \text{ keV}} \right]^4 \\ &\quad \left[\frac{d}{100 \text{ kpc}} \right]^{-2} \left[\frac{M_{DM, FoV}}{10^7 M_\odot} \right] \frac{\text{ph}}{\text{cm}^2 \text{s}} \end{aligned} \quad (3)$$

Note, that the flux (3) does not depend on the exact DM distribution, but only on the total mass inside the telescope's FoV. The latter can be measured with greater accuracy than the measurement of a profile. The uncertainty in the expected DM decay flux (3) can be directly propagated from the uncertainties in M_{DM} measurements.

In our work we consider the sample of dwarf spheroidal galaxies presented by Wolf et al. [27], where the authors obtained accurate estimates of the DM mass inside the half-light radius, i.e. the radius within which half of the total light is observed. The choice of this integration radius is motivated by the fact that this radius minimizes the uncertainty in the enclosed mass. In Table I we summarize the available data on dSphs for which archival XMM-Newton data are available. These data (from Wolf et al. [27]) quote the mass estimates $M_{1/2}$ within the half-light radius, together with the uncertainties and the values of the half-light radius both in physical distance ($r_{1/2}$) and apparent opening angle ($\theta_{1/2}$). For a number of dSphs (e.g. Ursa Minor), the half-light radius exceeds the size of the XMM-Newton FoV, $\theta_{FoV} \simeq 15'$. This implies that only a fraction of the DM decay signal is visible in a single XMM-Newton pointing. In what follows we take this effect into account for the estimation of the DM flux from these particular galaxies. Namely, we assume that the mass within the FoV scales as $M_{DM, FoV} \sim \theta_{FoV}$ for the sources with $\theta_{1/2} > \theta_{FoV}$, taking into account the fact that the velocity dispersion profiles of dSphs are flat, see e.g. Walker et al. [28], Walker [29] and references therein.

B. Milky Way

The DM decay flux from the Milky Way halo is typically comparable to the flux from isolated distant sources, like dSph galaxies or galaxy clusters [30]. The flux from DM decay in the Milky Way within the telescope field-

of-view Ω_{FoV} ,

$$F = \frac{\Gamma \Omega_{FoV} \mathcal{S}}{4\pi m_{DM}} \quad (4)$$

is determined by the column density of the DM

$$\mathcal{S} = \int_0^\infty \rho_{DM} \left(\sqrt{r_\odot^2 - 2zr_\odot \cos \phi + z^2} \right) dz \quad (5)$$

where $r_\odot = 8.5 \text{ kpc}$ is the distance from the Sun to the centre of our Galaxy and the angle ϕ relates to the galactic coordinates (l, b) as $\cos \phi = \cos b \cos l$.

For a source of angular size θ , the contribution of the MW to the DM decay flux is

$$\begin{aligned} F_{MW} &= 1.1 \times 10^{-6} \left[\frac{\theta}{\theta_{FoV}} \right]^2 \left[\frac{S}{10^{22} \text{ GeV/cm}^2} \right] \\ &\quad \left[\frac{\theta_{DM}^2}{1.75 \times 10^{-11}} \right] \left[\frac{m_{DM}}{7.1 \text{ keV}} \right]^4 \text{ ph/cm}^2 \text{ s} \end{aligned} \quad (6)$$

To estimate the column density S of Galactic DM in different directions, we adopt the models of the DM halo of the Milky Way discussed by Klypin et al. [31]. Klypin et al. [31] have adopted the Navarro-Frenk-White (NFW, Navarro et al. [32]) profile

$$\rho_{NFW}(r) = \frac{\rho_s r_s^3}{r(r+r_s)^2} \quad (7)$$

in which the characteristic density ρ_s and radius r_s are free parameters estimated from the data.

The uncertainty in the column density as well as in the radial DM density profile arises from the difficulty of disentangling contributions from the visible and DM components to the Galaxy rotation curve. In what follows we consider the ‘‘favoured NFW’’ model of Klypin et al. [31] for the estimate of the *mean* Milky Way DM column density in the direction of individual dSphs (with $\rho_s = 4.9 \times 10^6 M_\odot \text{ kpc}^{-3}$, $r_s = 21.5 \text{ kpc}$). To estimate how the uncertainty propagates to the limits on the mixing angle of sterile neutrino DM, we also consider the column densities of Galactic DM deduced from the ‘‘maximal disk model’’ ($\rho_s = 0.6 \times 10^6 M_\odot \text{ kpc}^{-3}$, $r_s = 46 \text{ kpc}$) of Klypin et al. [31]. We refer to this estimate as the *minimal* Galactic DM contribution to the signal. For each position in the sky the *minimal* DM column density is 2-3 times lower than the estimated *mean* column density.

The expected Galactic contribution to the DM decay flux from individual dSphs is given in Table II. The total expected DM decay flux from the direction of each dSph galaxy is the sum of the fluxes given in Eqs. (3) and (6).

III. OBSERVATIONS AND DATA ANALYSIS

The details of the XMM-Newton observations of the dSph galaxies selected for this analysis are summarized

Name	d kpc	$M_{1/2}$ $10^7 M_\odot$	$r_{1/2}$ kpc	$\theta_{1/2}$ arcmin
Carina	105 ± 2	$0.95^{+0.095}_{-0.09}$	0.334	10.9
Draco	76 ± 5	$2.11^{+0.31}_{-0.31}$	0.291	13.2
Fornax	147 ± 3	$7.39^{+0.41}_{-0.36}$	0.944	22.1
Leo I	254 ± 18	$2.21^{+0.24}_{-0.24}$	0.388	5.3
Ursa Minor	77 ± 4	$5.56^{+0.79}_{-0.72}$	0.588	26.3
Ursa Major II	32 ± 4	$0.79^{+0.56}_{-0.31}$	0.184	19.8
Willman I	38 ± 7	$0.04^{+0.02}_{-0.02}$	0.033	3.0
NGC 185	616 ± 26	$29.3^{+10.2}_{-7.7}$	0.355	2.0

TABLE I: Parameters of dwarf spheroidal galaxies considered in the analysis. The data is taken from Wolf et al. [27].

Object	Exposure,	F_{dSph} ,	$F_{MW,mean}$	$F_{MW,min}$
	$10^7 \text{ cm}^2 \text{ s}$	$10^{-7} \text{ cts/cm}^2/\text{s}$	$10^{-7} \text{ cts/cm}^2/\text{s}$	$10^{-7} \text{ cts/cm}^2/\text{s}$
Carina	1.41	$2.1^{+0.21}_{-0.20}$	5.9	2.7
Draco	6.23	$8.8^{+1.3}_{-1.3}$	9.8	4.4
Fornax	5.35	$5.6^{+0.31}_{-0.27}$	10.8	5.0
Leo	5.03	$0.8^{+0.09}_{-0.09}$	1.2	0.56
NGC185	12.75	$1.9^{+0.66}_{-0.50}$	0.4	0.15
UMa II	0.87	$14.0^{+9.92}_{-5.50}$	8.7	4.2
UMi	0.86	$12.8^{+1.82}_{-1.66}$	11.0	5.0
Willman	8.36	$0.7^{+0.35}_{-0.35}$	0.4	0.2
TOTAL	40.86	$3.55^{+0.79}_{-0.63}$	3.9	1.8

TABLE II: Expected fluxes from DM decay line with parameters corresponding to Bulbul et al. [1]. For each dwarf spheroidal galaxy the expected flux is split into two components: the signal from the dwarf itself (F_{dSph} , see Eq. 3) and from the Milky Way (F_{MW} , see Eq. 6). For the MW contribution flux estimates are given for both mean and minimal DM profiles.

in Table III. We collected all publicly-available observations of eight dSphs with exposures exceeding 10 ks. The total exposure time of the observations is ~ 0.6 Msec. In most cases, the observations were already used for the search of the DM decay signal and upper bounds on the sterile-neutrino DM mixing angle were already derived on a source-by-source basis [21–23]. The goal of our re-analysis of these data is to stack the signal from all the dSphs to increase our sensitivity to the DM decay line.

We processed the raw data with the ESAS (v.0.9.28 as part of XMM SAS v.13.5) reduction scheme [33][41] using the calibration files from May 2014. Within this scheme, we produced cleaned event files by removing the periods of soft proton flares. After the flare removal, we performed a self-consistency check on the level of contribution of residual soft protons to the background flux, following Leccardi and Molendi [34]. This contribution is found to be less than $\sim 20\%$ in all observations. In any case, the spectrum of the soft protons is featureless, so our line search is unaffected by soft-proton contamination.

Obs Id	Name	Duration, ksec	Clean exposure, ksec
0200500201	Carina	41.9	19.2+16.7+8.4
0603190101	Draco	19.0	17.5+17.9+14.3
0603190201	Draco	19.9	18.5+18.2+14.7
0603190301	Draco	17.7	12.2+12.6+6.3
0603190501	Draco	19.9	18.6+18.5+14.9
0302500101	Fornax	103.9	65.1+65.9+53.0
0555870201	Leo	94.0	75.4+77.1+0
0652210101	NGC 185	123.5	91.4+96.2+66.7
0650180201	UMa II	34.3	11.7+12.5+7.4
0301690401	UMi	11.8	10.8+10.9+7.9
0652810101	Willman	29.3	15.0+19.0+9.5
0652810301	Willman	36.0	21.9+23.2+15.5
0652810401	Willman	36.2	27.5+28.5+16.2
TOTAL		602.3	404.8+417.2+232.8

TABLE III: XMM-Newton observations of dwarf spheroidals considered in this analysis. The total exposure time is given as the sum of effective exposures for the MOS1, MOS2 and pn cameras individually. The total clean exposure is ~ 0.6 Msec

We masked all the detected point sources in the FoV using the ESAS task `cheese`, such that only the signal from the extended DM halo of the dSphs is taken into account. We then extracted spectra and images of the extended emission using the ESAS tasks `mos-spectra` and `pn-spectra`. These tools use a collection of closed-filter data to estimate the local non X-ray background (NXB) by scaling the normalization of the closed-filter spectra to match the count rates measured in the unexposed corners of each of the three EPIC detectors.

We stacked the spectra of all the dSph observations using the `addspec` routine, to obtain mean MOS1+MOS2 and pn spectra. We then fitted the resulting spectra in the 0.7-10 keV energy band with the sum of models representing the astrophysical and NXB contributions. We ignored the energy interval 1.2-1.8 keV from the fit, as this range is affected by the presence of strong and time-variable Si $K\alpha$ and Al $K\alpha$ fluorescence lines.

Instead of subtracting the NXB spectra directly from the data, we modelled the NXB spectrum using a phenomenological model including all known fluorescence lines (see Appendix B of Leccardi and Molendi [34]) and added this model as an additive component to the fit. This method has the advantage of retaining the original statistics of the spectrum and allowing for possible variations of the NXB level, e.g. caused by soft protons. During the fitting procedure, we fixed the spectral shape of the particle-induced continuum to the values obtained from the closed-filter data, since this component is known to be stable with time [34]. On the other hand, we leave the normalizations of the instrumental lines free while fitting. In the case of the pn camera we also need to model the Ca line at ~ 4.6 keV. We note that no instrumental line is observed between 3 and 4 keV, thus this analysis is suitable for the detection of an additional emission

Model name	Parameter	Value	Error
apec1	kT,keV	0.91	0.05
apec1	norm	$3.5 \cdot 10^{-5}$	$0.5 \cdot 10^{-5}$
apec2	kT, keV	0.35	0.06
apec2	norm	$2.9 \cdot 10^{-5}$	$0.7 \cdot 10^{-5}$
powerlaw	PhoIndex	1.34	0.05
powerlaw	norm	$1.2 \cdot 10^{-4}$	$6.0 \cdot 10^{-6}$

TABLE IV: Parameters of the fit of the stacked spectra of dSphs with the reference background model.

line in this energy range. For the details of the analysis procedure, we refer the reader to Eckert et al. [35].

The astrophysical background and foreground contribution is modelled as the sum of a power law representing the cosmic X-ray background (CXB) and two *apec* models for the Galactic emission. The combined fit is reasonably good, with $\chi^2/DOF = 595.5/576$. In Fig. 1 we show the stacked spectra and best-fit model for pn (red) and MOS (black). The residuals from the fit are displayed in the bottom panel of the figures. The main parameters of the fit are given in Table IV. The fit requires the presence of a rather hot component at the temperature of ~ 0.9 keV, which is significantly higher than the typical temperature [36]; however the temperature of the Galactic halo is known to vary significantly from one direction to another, and thus such a result is not unusual [37]. In any case, we note that the foreground emission from the MW halo is very soft compared to the energy range of interest for this study (see Fig. 1), such that the exact temperature of the foreground component has little influence on our analysis. Moreover, the spectral slope of the CXB, which is the dominant sky component beyond ~ 1 keV, is in excellent agreement with the canonical value of 1.4 [e.g. 38]. The normalization of the CXB in each individual observation was also found to agree with the measurement of De Luca and Molendi [38]. A closer look at the residuals in the range of interest for this analysis, i.e. the range between 2 and 4 keV, is shown in Fig. 2.

To search for the DM decay line, we added to the model a narrow gaussian line at a fixed energy of 3.55 keV. The addition of such a line does not provide a significant improvement to the fit. To compute upper limits to the line flux marginalizing over all uncertainties, we sampled the likelihood using a Markov chain Monte Carlo (MCMC) method as implemented in XSPEC v12.8. After an initial burning phase of 5,000 steps, we performed 50,000 MCMC steps and drew the posterior distributions from the resulting chain. The output distribution for the line flux is shown in Fig. 3. From this distribution we obtained upper limits to the line flux of 2.54×10^{-7} phot $\text{cm}^{-2} \text{s}^{-1}$ (90% confidence level) and 3.98×10^{-7} phot $\text{cm}^{-2} \text{s}^{-1}$ (3σ). In addition, we also performed a search for the DM decay line in the entire energy range 2-10 keV, which did not give any positive results. From this analysis we derived an energy-dependent upper bound on the line flux.

The contribution of the individual dSph galaxies to the XMM-Newton signal could be calculated using the information on the instrument effective area A_i (found using the *plot efficiency* command in XSPEC) and the clean exposure t_i in each observation. If the expected flux of the DM decay line in the i th observation is F_i , the expected number of DM decay photons is $N_i = F_i A_i t_i$. The mean DM decay flux in the entire stacked dataset is then

$$\langle F \rangle = \frac{\sum_i F_i A_i t_i}{\sum_i A_i t_i}, \quad (8)$$

with the sum being performed over all dSph observations.

Table II gives the information on A_i and t_i in each observation, together with the estimate of the expected DM decay line flux calculated assuming the sterile neutrino DM parameters suggested by the observations of Bulbul et al. [1].

IV. RESULTS AND DISCUSSION

Our analysis of the stacked sample of dSph galaxies provides a moderate improvement of constraints on the parameters for sterile neutrino DM, compared to the previously-derived bounds based on the previous observations of the diffuse X-ray background, of individual dSph galaxies, of the Milky Way and of galaxy clusters.

As it follows from Table II, the flux from DM decay expected to be seen in the combination of observations of all dwarves is $F_{mean} \sim 7.4 \pm 0.7 \times 10^{-7}$ cts/s/cm² for mean dark matter column density in the MW and $F_{min} \sim 5.3 \pm 0.7 \times 10^{-7}$ cts/s/cm² for minimal Galactic DM column density. Such a flux was expected to be detected at 4.6σ or 3.3σ levels for the mean / minimal Galactic DM column density models in the stacked dSph dataset. The non-detection of the DM line in the analyzed data sets is, therefore, inconsistent with the assumption that the unidentified line at 3.55 keV is produced by decaying sterile-neutrino DM with parameters suggested by the analysis of Bulbul et al. [1].

This is illustrated by Fig. 4, where we plot the 2σ upper limits on the mixing angle of the DM sterile neutrino as a function of the DM particle mass. The value of $\sin^2(2\theta)$ derived by Bulbul et al. [1] is above the 2σ upper bound for both the *mean* and *minimal* Galactic DM column density models.

The calculation of the DM decay line flux from the direction of galaxy clusters by Bulbul et al. [1] does not include the flux from the foreground DM halo of the Milky Way. This is justified if the foreground flux is subtracted in the analysis of the spectra of the galaxy clusters. This is not the case in the analysis of Bulbul et al. [1], who modelled the cluster spectra together with the instrumental and sky background / foreground in a way similar to the approach adopted here. In this case, the flux from DM

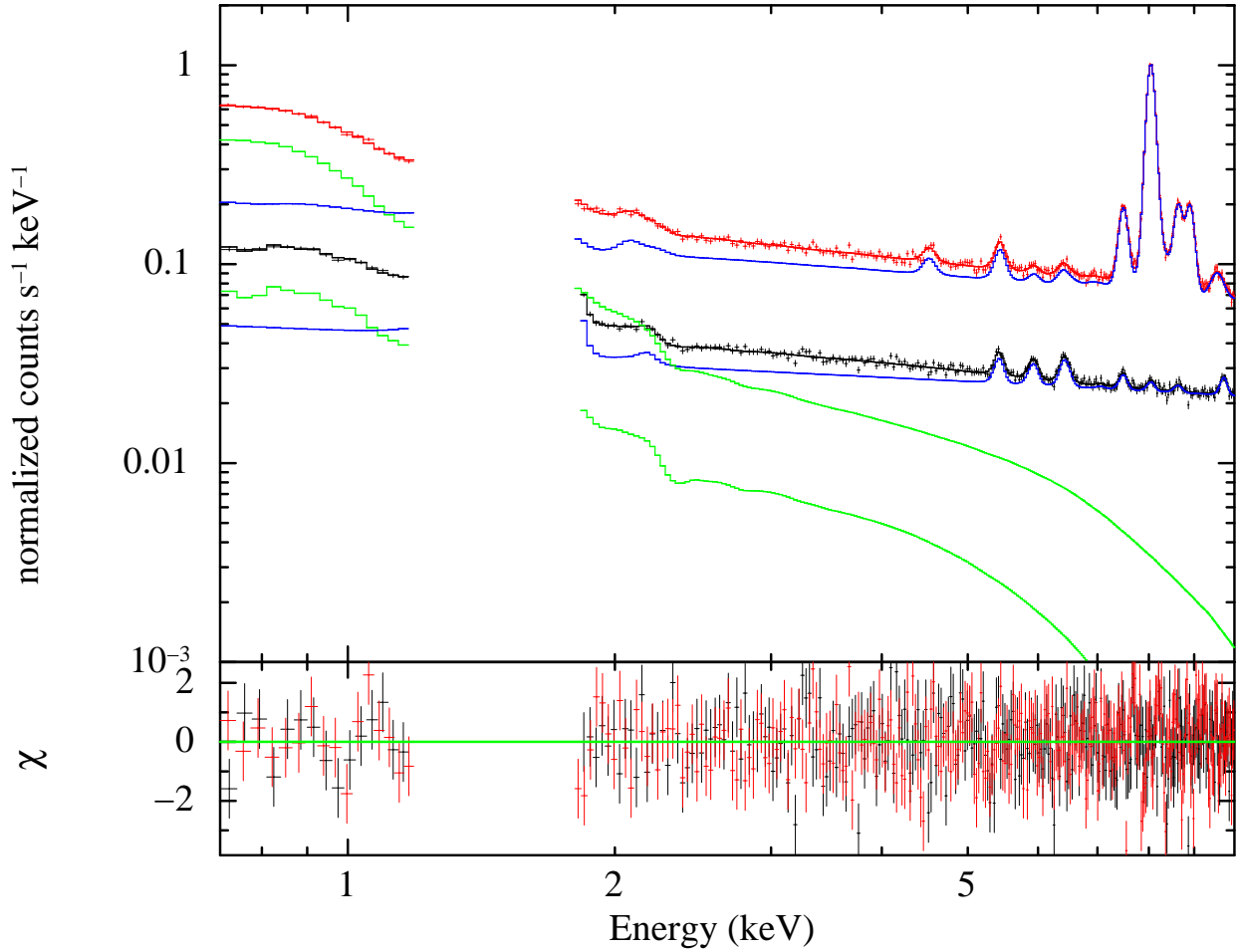


FIG. 1: MOS1+2 (black) and pn (red) stacked spectra of dSph galaxies. The top panel shows the data and the best-fit model, broken into the astrophysical contribution (green) and the NXB (blue), while the bottom panel shows the residuals from the model.

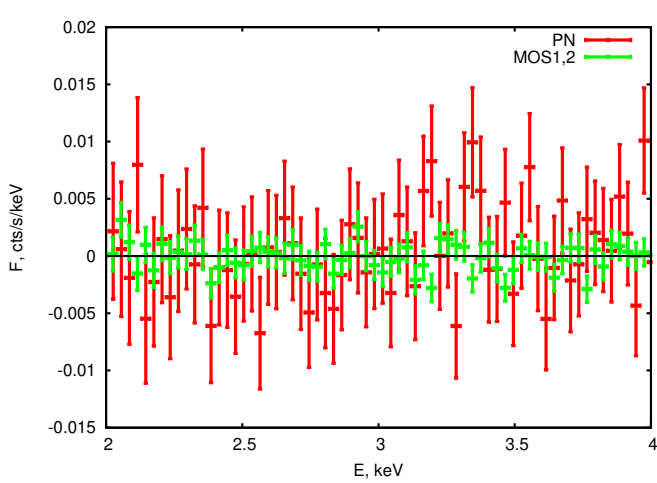


FIG. 2: Residual flux from the combined MOS 1,2 (green) and pn (red) cameras in the 2-4 keV energy band including the expected 3.55 keV line.

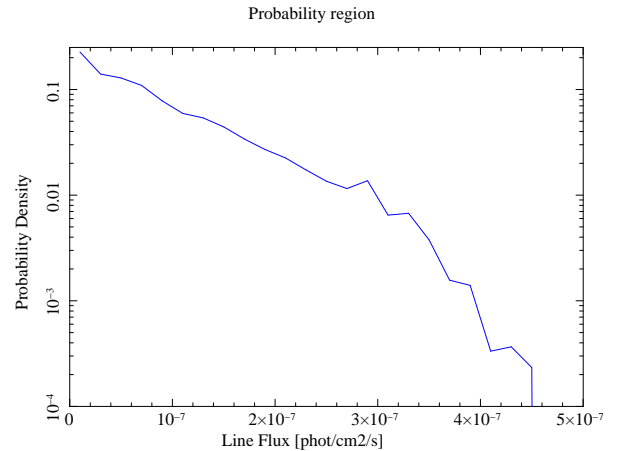


FIG. 3: Posterior probability distribution for the 3.55 keV line flux in the stacked dSph dataset, obtained through 50,000 MCMC sampling of the likelihood function.

decay in the MW halo should, in principle, be included

in the calculation of the line flux [39]. This should result in a somewhat lower value of the sterile neutrino mixing angle $\sin^2(2\theta^2)$ from the observed line flux. This effect

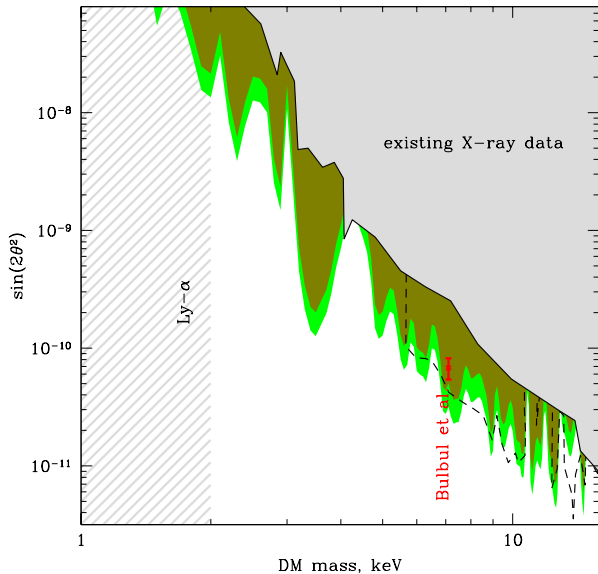


FIG. 4: Exclusion plot on sterile neutrino mass – mixing angle plane. All parameter values above the curves are excluded. The solid dark green and light green lines show the 2σ constraints for minimal and mean dark matter column density in the Milky Way, respectively. The red point with error bars indicates the parameter values reported by Bulbul et al. [1]. The dashed line indicates the M31 constraints from Horiuchi et al. [40].

might potentially relax the inconsistency of the Bulbul et al. [1] result with the dSph data reported here.

The estimates of $\sin^2(2\theta^2)$ derived by Boyarsky et al. [2] from the analysis of M31 and of the Perseus galaxy cluster are much more uncertain than those derived from the stacked galaxy cluster sample, because of the much larger uncertainty in the DM column density in the two particular individual sources. Taking into account a roughly order-of-magnitude uncertainty in the estimate of $\sin^2(2\theta^2)$ derived from the analysis of Boyarsky et al. [2], one could see that our constraints on the DM parameters derived from the dSph data are still consistent with the results of Boyarsky et al. [2].

Our analysis is only marginally ruling out the possibility of the DM decay origin of the unidentified line at 3.55 keV. An increase of the sensitivity by a factor of ~ 2 is necessary to firmly rule out the DM decay line hypothesis for the line origin. This is possible already with XMM-Newton (rather than with the next-generation telescopes like ASTRO-H), via a moderate increase of exposure towards selected dSph galaxies (e.g. Ursa Minor, Ursa Major II), which are characterized by strong DM decay line flux, but are currently not dominating the stacked dSph signal because of the relatively short exposures. Deeper XMM-Newton observations of these dSphs galaxies would thus be sufficient to test conclusively the DM origin of the 3.55 keV line.

-
- [1] E. Bulbul, M. Markevitch, A. Foster, R. K. Smith, M. Loewenstein, and S. W. Randall, ArXiv e-prints (2014), 1402.2301.
- [2] A. Boyarsky, O. Ruchayskiy, D. Iakubovskiy, and J. Franse, ArXiv e-prints (2014), 1402.4119.
- [3] A. Boyarsky, J. Franse, D. Iakubovskiy, and O. Ruchayskiy, ArXiv e-prints (2014), 1408.2503.
- [4] T. E. Jeltema and S. Profumo (2014), 1408.1699.
- [5] S. Dodelson and L. M. Widrow, Phys. Rev. Lett. **72**, 17 (1994), hep-ph/9303287.
- [6] T. Asaka, S. Blanchet, and M. Shaposhnikov, Phys. Lett. **B631**, 151 (2005), hep-ph/0503065.
- [7] M. Lattanzi and J. W. F. Valle, Phys. Rev. Lett. **99**, 121301 (2007), 0705.2406.
- [8] M. Shaposhnikov and I. Tkachev, Physics Letters B **639**, 414 (2006), hep-ph/0604236.
- [9] A. Boyarsky, A. Neronov, O. Ruchayskiy, and M. Shaposhnikov, MNRAS **370**, 213 (2006), astro-ph/0512509.
- [10] K. N. Abazajian, M. Markevitch, S. M. Koushiappas, and R. C. Hickox, Phys. Rev. D **75**, 063511 (2007), arXiv:astro-ph/0611144.
- [11] A. Boyarsky, A. Neronov, O. Ruchayskiy, and M. Shaposhnikov, Phys. Rev. D **74**, 103506 (2006), astro-ph/0603368.
- [12] S. Riemer-Sørensen, K. Pedersen, S. H. Hansen, and H. Dahle, Phys. Rev. D **76**, 043524 (2007), arXiv:astro-ph/0610034.
- [13] A. Boyarsky, O. Ruchayskiy, and M. Markevitch, ApJ **673**, 752 (2008), astro-ph/0611168.
- [14] C. R. Watson, J. F. Beacom, H. Yuksel, and T. P. Walker, Phys. Rev. **D74**, 033009 (2006), astro-ph/0605424.
- [15] A. Boyarsky, A. Neronov, O. Ruchayskiy, M. Shaposhnikov, and I. Tkachev, Phys. Rev. Lett. **97**, 261302 (2006), astro-ph/0603660.
- [16] A. Boyarsky, J. Nevalainen, and O. Ruchayskiy, A&A **471**, 51 (2007), astro-ph/0610961.
- [17] A. Boyarsky, D. Malyshev, A. Neronov, and O. Ruchayskiy, MNRAS **387**, 1345 (2008), 0710.4922.
- [18] H. Yuksel, J. F. Beacom, and C. R. Watson, Phys. Rev. Lett. **101**, 121301 (2008), 0706.4084.
- [19] A. Boyarsky, J. W. den Herder, A. Neronov, and O. Ruchayskiy, Astropart. Phys. **28**, 303 (2007), astro-ph/0612219.
- [20] A. Boyarsky, O. Ruchayskiy, M. G. Walker, S. Riemer-Sørensen, and S. H. Hansen, Mon.Not.Roy.Astron.Soc. **407**, 1188 (2010), 1001.0644.
- [21] S. Riemer-Sørensen and S. H. Hansen, A&A **500**, L37 (2009), 0901.2569.
- [22] M. Loewenstein, A. Kusenko, and P. L. Biermann, ApJ **700**, 426 (2009), 0812.2710.
- [23] M. Loewenstein and A. Kusenko, Astrophys.J. **751**, 82 (2012), 1203.5229.
- [24] A. Kusenko, M. Loewenstein, and T. T. Yanagida, ArXiv e-prints (2012), 1209.6403.

- [25] S. Riemer-Sorensen, ArXiv e-prints (2014), 1405.7943.
- [26] P. B. Pal and L. Wolfenstein, Phys. Rev. D **25**, 766 (1982).
- [27] J. Wolf, G. D. Martinez, J. S. Bullock, M. Kaplinghat, M. Geha, R. R. Muñoz, J. D. Simon, and F. F. Avedo, MNRAS **406**, 1220 (2010), 0908.2995.
- [28] M. G. Walker, M. Mateo, E. W. Olszewski, O. Y. Gnedin, X. Wang, B. Sen, and M. Woodroffe, ApJ **667**, L53 (2007), 0708.0010.
- [29] M. Walker, *Dark Matter in the Galactic Dwarf Spheroidal Satellites* (2013), p. 1039.
- [30] A. Boyarsky, A. Neronov, O. Ruchayskiy, M. Shaposhnikov, and I. Tkachev, Physical Review Letters **97**, 261302 (2006), astro-ph/0603660.
- [31] A. Klypin, H. Zhao, and R. S. Somerville, ApJ **573**, 597 (2002), astro-ph/0110390.
- [32] J. F. Navarro, C. S. Frenk, and S. D. M. White, ApJ **490**, 493 (1997), astro-ph/9611107.
- [33] S. L. Snowden, R. F. Mushotzky, K. D. Kuntz, and D. S. Davis, A&A **478**, 615 (2008), 0710.2241.
- [34] A. Leccardi and S. Molendi, A&A **486**, 359 (2008), 0804.1909.
- [35] D. Eckert, S. Molendi, M. Owers, M. Gaspari, T. Venturi, L. Rudnick, S. Etori, S. Paltani, F. Gastaldello, and M. Rossetti, ArXiv e-prints (2014), 1408.1394.
- [36] D. McCammon, R. Almy, E. Apodaca, W. Bergmann Tiest, W. Cui, S. Deiker, M. Galeazzi, M. Juda, A. Lesser, T. Mihara, et al., ApJ **576**, 188 (2002), astro-ph/0205012.
- [37] K. Masui, K. Mitsuda, N. Y. Yamasaki, Y. Takei, S. Kimura, T. Yoshino, and D. McCammon, PASJ **61**, 115 (2009).
- [38] A. De Luca and S. Molendi, A&A **419**, 837 (2004), astro-ph/0311538.
- [39] A. Boyarsky, A. Neronov, O. Ruchayskiy, M. Shaposhnikov, and I. Tkachev, Physical Review Letters **97**, 261302 (2006), astro-ph/0603660.
- [40] S. Horiuchi, P. J. Humphrey, J. Oñorbe, K. N. Abazajian, M. Kaplinghat, and S. Garrison-Kimmel, Phys. Rev. D **89**, 025017 (2014), 1311.0282.
- [41] See e.g. <http://heasarc.gsfc.nasa.gov/docs/xmm/esas/esasimage/esas>